THE JOURNAL OF PHYSICAL CHEMISTRY B LETTERS

2006, *110,* 14055−14059
Published on Web 07/01/2006

Photoinduced Charge Separation in Titania Nanotubes

Takashi Tachikawa, Sachiko Tojo, Mamoru Fujitsuka, Toru Sekino, and Tetsuro Majima*

The Institute of Scientific and Industrial Research (SANKEN), Osaka University, Mihogaoka 8-1, Ibaraki, Osaka 567-0047, Japan

Received: June 19, 2006; In Final Form: June 20, 2006

The photocatalytic one-electron oxidation reaction of an aromatic compound during UV light irradiation of titania nanotubes and nanoparticles was investigated using time-resolved diffuse reflectance spectroscopy. Remarkably long-lived radical cations of the aromatic compound and trapped electrons were observed for the nanotubes when compared to those for nanoparticles. The influences of the morphology on the one-electron oxidation process of an aromatic compound adsorbed on the surface were discussed in terms of the charge recombination dynamics between the radical cation and electrons in TiO_2.

Introduction

Low dimensional TiO_2 nanostructures, such as nanotubes, nanofibers, and nanowires, have attracted much attention in recent years, because they have potential applications in photocatalysts, gas sensors, solar energy conversion, and so on.[1−12] In particular, TiO_2 nanotubes have a high specific surface area available for the adsorption of a dye sensitizer compared to bulk materials or nanoparticles, and they also provide channels for enhanced electron transfer, thereby helping to increase the efficiencies of solar cells.[8−10] Both the high amount of adsorbates and the efficient charge separation should play important roles in the one-electron oxidation reactions of organic molecules during the photocatalytic reactions. The small particle size tends to increase the photocatalytic activity of TiO_2 due to the high number of surface sites for adsorption, although there might be limits to this beneficial effect since the recombination rate of the photogenerated electrons (e^-) and holes (h^+) may be high in extremely small particles. These fast charge transfer and recombination kinetics have been studied in detail by several groups.[13−17] However, the increased delocalization of charge carriers in nanotubes, where they are free to move throughout the length of the crystal, is expected to reduce the recombination probability.

As is well-known, the charge recombination process plays an important role in the efficiency of the photocatalytic reactions.[18,19] Although there have been a great number of studies,[1−12] only a few quantitative studies have been reported for the photocatalytic reactions of such low dimensional TiO_2 nanomaterials. Furthermore, to the best of our knowledge, there is no report related to these issues using a time-resolved technique.

Herein, for the first time, we investigated the influences of the morphology on the charge separation and recombination processes of the photogenerated charge carriers using nanosecond time-resolved diffuse reflectance spectroscopy. Time-resolved diffuse reflectance spectroscopy is a powerful tool for the investigation of photocatalysis under various conditions.[20−27] To estimate the one-electron oxidation reactivities of the photogenerated h^+, we selected 4-(methylthio)phenyl methanol (MTPM) as the substrate due to the specific spectroscopic properties of MTPM and the MTPM radical cation ($MTPM^{\bullet+}$), which have a negligible absorption at 355 nm as the excitation wavelength for TiO_2 and absorption in the visible region (abound 400−600 nm), respectively.[25,26] The relationship between the concentration of $MTPM^{\bullet+}$ and the amount of adsorbed MTPM (n_{ad}) on the surface was examined. We also studied the photocatalytic degradation of carbon tetrachloride (CCl_4) by monitoring the bleaching of the absorption band due to the trapped e^- in TiO_2 from the steady-state diffuse reflectance measurements. Finally, the influence of the morphology on the photocatalytic degradation processes of an organic compound was discussed in terms of the charge recombination dynamics between the radical cation and e^- in TiO_2.

Experimental Methods

Materials. The TiO_2 nanoparticle powders were supplied by Ishihara Sangyo (ST-01, ST-21, and ST-41). These photocatalysts have a Brunauer−Emmett−Teller (BET) surface area of 300, 50, and 10 $m^2\ g^{-1}$, a primary particle size of about 7, 20, and 200 nm, and a crystal structure of 100% anatase, respectively.

The TiO_2 nanotubes were prepared by following the procedure described by Kasuga and co-workers.[1] In a typical method, the anatase TiO_2 powder (Kojundo Chemical Laboratory) was added to a 10 M NaOH solution and heated for 20 h at 150 °C. The white, powdery TiO_2 was thoroughly washed with 0.1 M HCl aqueous solution, distilled water, and ethanol, followed by drying at 80 °C. The nanotubes (denoted as TNT-as prepared in this text) were then annealed in air at 400 °C for 3 h, which became the high crystalline TiO_2 nanotubes (denoted as TNT-400 in this text).

Examination of the morphology and characterization of the powders were performed using a high-resolution transmission

* To whom correspondence should be addressed. Tel: +81-6-6879-8495. Fax: +81-6-6879-8499. E-mail: majima@sanken.osaka-u.ac.jp.

10.1021/jp063800q CCC: $33.50

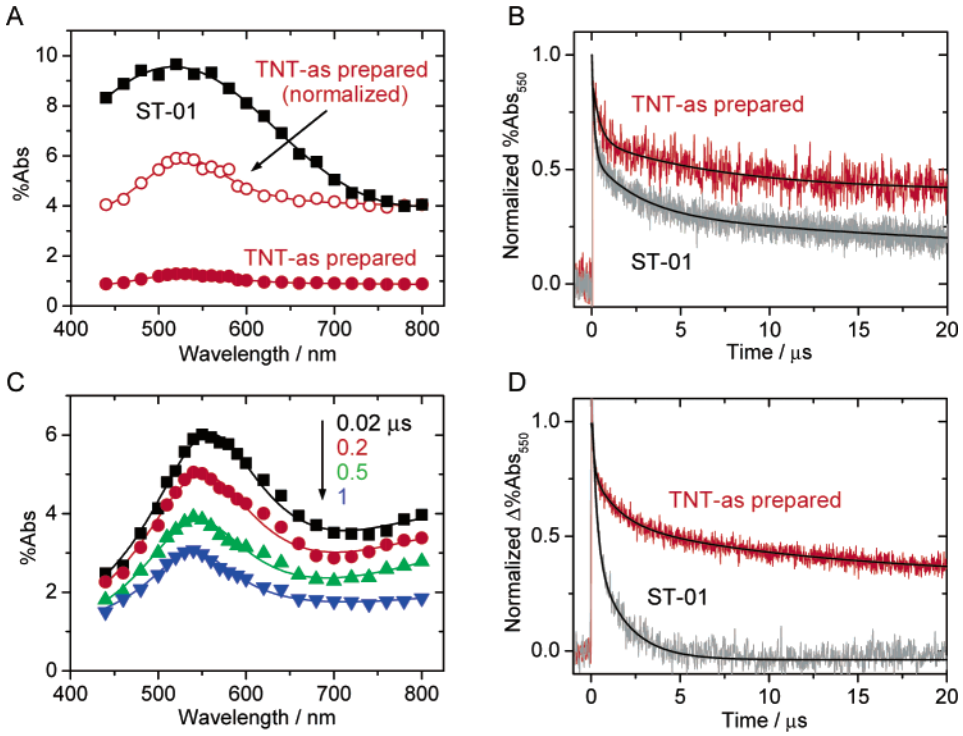

Figure 1. (A) Time-resolved diffuse reflectance spectra observed at 0.1 μs after the laser flash for ST-01 and TNT-as prepared in aerated CH_3CN. (B) Time traces at 550 nm observed for ST-01 and TNT-as prepared in CH_3CN. The solid black line is obtained by curve fitting with the multiexponential functions. (C) Time-resolved diffuse reflectance spectra observed after the laser flash for TNT-as prepared in the presence of MTPM (10 mM) in CH_3CN. (D) Differential time traces of %Abs at 550 nm obtained by subtracting the time trace observed in the absence of MTPM from that observed in the presence of MTPM (10 mM) for ST-01 and TNT-as prepared in CH_3CN.

electron microscope (TEM, Hitachi H8100) and an energy-dispersive X-ray spectrometer (EDS) attached to the TEM.[1] The precipitated crystals were analyzed using a powder X-ray diffractometer (XRD, Rigaku Rint-1000). The nanotubes (anatase phase) were found to have a hollow structure with a typical outer diameter of about 7−10 nm, inner diameter of 5−7 nm, and length of several hundred nm (Figure S1). There are no clear differences in the physical appearance of the TNT-as prepared and TNT-400 (Figure S1), although the structure was changed into a rodlike structure by annealing at >500 °C. The tube axis is along the [010] direction of the anatase phase. The specific surface areas were determined by the BET method.

4-(Methylthio)phenyl methanol (MTPM) (Aldrich) was purified by vacuum sublimation before use. Fresh acetonitrile (CH_3CN) (Nacalai Tesque, spectral grade) was used as the solvent without further purification. Carbon tetrachloride (CCl_4) (Wako) was used as the electron scavenger without further purification. The sample suspensions containing the TiO_2 powder (20 g dm^{-3}) were sonicated for 10 min before the spectral measurements.[25,26]

Steady-State and Time-Resolved Diffuse Reflectance Spectral Measurements. The steady-state UV−visible diffuse reflectance spectra were measured using UV−visible−NIR spectrophotometers (Jasco, V-570) at room temperature.

The time-resolved diffuse reflectance measurements were performed using the third harmonic generation (355 nm, 5 ns full width at half-maximum) from a Q-switched Nd^{3+}:YAG laser (Continuum, Surelite II-10) for the excitation operated by temporal control using a delay generator (Stanford Research Systems, DG535). The reflected analyzing light from a pulsed 450-W Xe-arc lamp (Ushio, UXL-451-0) was collected by a focusing lens and directed through a grating monochromator (Nikon, G250) to a silicon avalanche photodiode detector (Hamamatsu Photonics, S5343). The transient signals were recorded by a digitizer (Tektronix, TDS 580D). All experiments were carried out at room temperature.

The reported signals are the averages of 10−30 events. The % absorption (%Abs) is given by eq 1

$$\%\ \mathrm{Abs} = \frac{R_0 - R}{R_0} \times 100 \qquad (1)$$

where R and R_0 represent the intensities of the diffuse reflected monitor light with and without excitation, respectively.[20,21] The linearity between %Abs and the concentration of the transient species can be satisfied only when %Abs is below 10% as suggested elsewhere.[22]

Results and Discussion

Figure 1A shows the time-resolved diffuse reflectance spectra observed after the laser flash during the 355-nm laser photolysis (1.5 mJ $pulse^{-1}$, 5 ns fwhm) of the TNT-as prepared and ST-01 powders slurried in aerated CH_3CN. According to the literature,[16,17,27] a broad transient absorption band with a maximum around 520 nm that appeared after the laser flash was assigned to the trapped h^+. For the TNT-as prepared, the absorption band attributed to the trapped h^+ was much smaller than that for ST-01, when the %Abs values are normalized at 800 nm assigned to the trapped e^-. This suggests that the number of h^+ trapping sites on the surface of the TNT-as prepared are much less than that of ST-01.

As summarized in Table 1, the apparent quantum yields of the charge separation (ϕ_{CS}), which is determined from the absorbed photon numbers and initial %Abs ($\%Abs^{t=0}$) values observed at 550 nm,[28] which are mainly assigned to the trapped h^+, decreased in the order of ST-01 > ST-21 > TNT-400 > ST-41 > TNT-as prepared. Notably, an obvious enhancement

TABLE 1: Diameter and BET Surface Area of TiO_2 Powders, Relative Apparent Yield of Charge Separation (ϕ_{rel}^{CS}), the Half-Lives of Transient Species ($t_{1/2}$), and the Lifetimes of Trapped e^- in TiO_2 (τ_e)

TiO_2	diameter, nm	BET surface area, $m^2\ g^{-1}$	ϕ_{rel}^{CS} [d]	$t_{1/2}^{CR}$, μs [e]	$t_{1/2}^{\bullet+}$, μs [f]	$t_{1/2}^{e}$, μs [g]	τ_e, min [h]
TNT-as prepared	>200[a,b]	309[b]	1.0	4.1 ± 0.6	4.0 ± 0.5	8 ± 3	N. A.
TNT-400	>200[a,b]	225[b]	2.0	3.5 ± 0.4	2.3 ± 0.4	12 ± 3	7.6[i], 55[j]
ST-01	7[c]	300[c]	7.1	0.6 ± 0.2	0.5 ± 0.1	0.7 ± 0.2	N. A.
ST-21	20[c]	50[c]	4.8	1.0 ± 0.2	1.0 ± 0.2	1.1 ± 0.2	N. A.
ST-41	200[c]	10[c]	1.6	0.7 ± 0.2	0.7 ± 0.2	N. A.	N. A.

[a] Length. [b] This work. [c] From manufacture's specifications. [d] Determined from the %Abs values at 550 nm observed at 50 ns after the laser flash. [e] The $t_{1/2}$ values observed for the charge recombination process, where $t_{1/2}$ is the time required for 50% of the initial %Abs values ($\%Abs^{t=0}$). [f] The $t_{1/2}$ values observed at 550 nm, which is mainly assigned to $MTPM^{\bullet+}$, during the 355-nm laser photolysis of TiO_2 powders in the presence of MTPM (10 mM). [g] The $t_{1/2}$ values observed at 760 nm, which is mainly assigned to the trapped e^- in TiO_2, during the 355-nm laser photolysis of TiO_2 powders in the presence of MTPM (10 mM) in aerated CH_3CN. [h] Fitted with a single-exponential decay function. [i] In aerated CH_3CN. [j] In aerated CH_3CN containing MTPM of 10 mM.

in ϕ_{CS} was observed for TNT-400, compared to that of the TNT-as prepared. This would be due to the improvement in the crystallinity of the anatase nanotubes (Figure S1). In addition, relatively long half-lives ($t_{1/2}$) of the charge carriers were observed for nanotubes when compared to those for nanoparticles (Figure 1B and Table 1). The observed time profiles cannot be fit with a simple single-exponential decay function. The nonexponential decay profile of the recombination can be explained using the model of recombination kinetics based on detrapping from deep traps.[29,30] Therefore, the observed non-exponential decay kinetics clearly indicates that the recombination rates are limited by the motion of the charge carriers in the particles. In the case of nanoparticles, i.e., the ST-series catalysts, the fact that almost the same $t_{1/2}$ values were observed would be related to the density and distribution of the trap sites at the surface and/or the impurity distribution in the particles.[31]

One would expect that the increase in $t_{1/2}$ of the charge carriers can enhance the one-electron oxidation efficiency of the organic compounds. To compare the one-electron oxidation efficiency between nanoparticles and nanotubes, we used 4-(methylthio)phenyl methanol (MTPM) as the substrate. We assumed that the photogenerated h^+ is the main oxidizing species as given by eq 2[25,26]

$$h^+ + MTPM \rightarrow MTPM^{\bullet+} \qquad (2)$$

Figure 1C shows the transient spectra obtained during the 355-nm laser photolysis of the TNT-as prepared in the presence of MTPM (10 mM) in aerated CH_3CN. A transient absorption band with a peak around 550 nm was obtained and assigned to $MTPM^{\bullet+}$.[25,26]

It should be noted that remarkably long $t_{1/2}$ values of $MTPM^{\bullet+}$ were observed for nanotubes when compared to those for nanoparticles (Figure 1D). Our experimental results suggest that the electron transport properties, such as a diffusion coefficient or a lifetime, are quite different between each other, because $MTPM^{\bullet+}$ is localized at the surface. Recently, Yanagida et al. have investigated the photoinjected electron transport in the TiO_2 nanotube electrodes and revealed that the higher efficiency resulted from an increase in the electron density by keeping a much longer lifetime in the nanotube electrodes than in the TiO_2 nanoparticle (Degussa P-25) electrodes.[10] Taking into the account that the diffusion coefficients for the nanotubes and nanoparticles are nearly the same,[10] we can consider that the observed increase in $t_{1/2}$ of $MTPM^{\bullet+}$ for the nanotube is due to the longer diffusion length (>200 nm), which results in the efficient charge separation when compared to those of the nanoparticles (7∼200 nm).

Recently, we found that the initial concentration of the radical cations generated from the one-electron oxidation reaction with h^+ significantly depends on the amount of adsorbates (n_{ad}).[24−26]

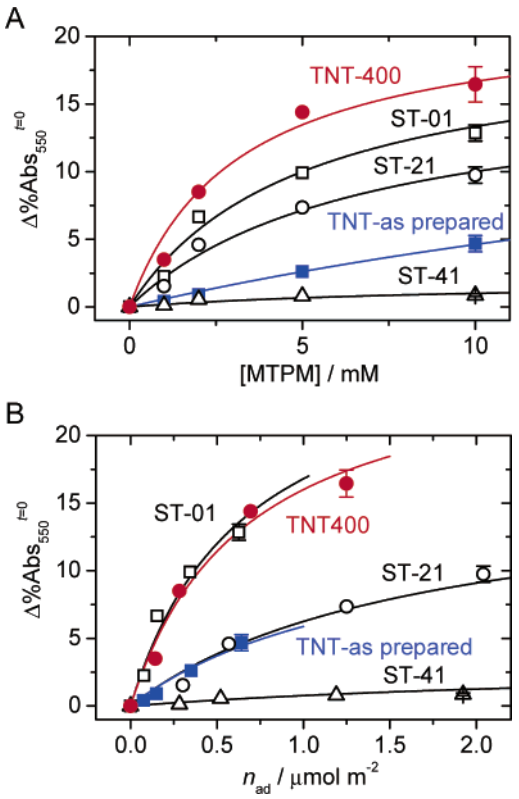

Figure 2. Relationship of $\Delta\%Abs^{t=0}$ with the initial MTPM concentration ([MTPM]) (A) and the amount of adsorbed MTPM (n_{ad}) (B).

Considering n_{ad} and $\Delta\%Abs^{t=0}$, which is obtained by subtracting %Abs observed immediately after the flash in the absence of MTPM from that observed in the presence of MTPM, we can compare the one-electron oxidation efficiency of the adsorbed MTPM.

As shown in Figure 2, panels A and B, a relatively low one-electron oxidation efficiency was obtained for the TNT-as prepared despite its high BET surface area (Table 1). On the other hand, a significant enhancement in the one-electron oxidation efficiency was observed for TNT-400. This is partially due to an increase in n_{ad} (Figure S2 and Table S1), which would be attributable to a decrease in the amount of adsorbed water or an increase in the number of defect sites on the surface by annealing of the nanotubes.[32] It is well-known that the defect sites on the TiO_2 surface play an important role in the adsorption of aliphatic alcohols and the alkoxide coverage increases by the creation of defects.[33,34]

Band gap excitation resulted in the one-electron oxidation of the substrate adsorbed on the TiO_2 surface, and continued photolysis led to the appearance of the well-known absorption

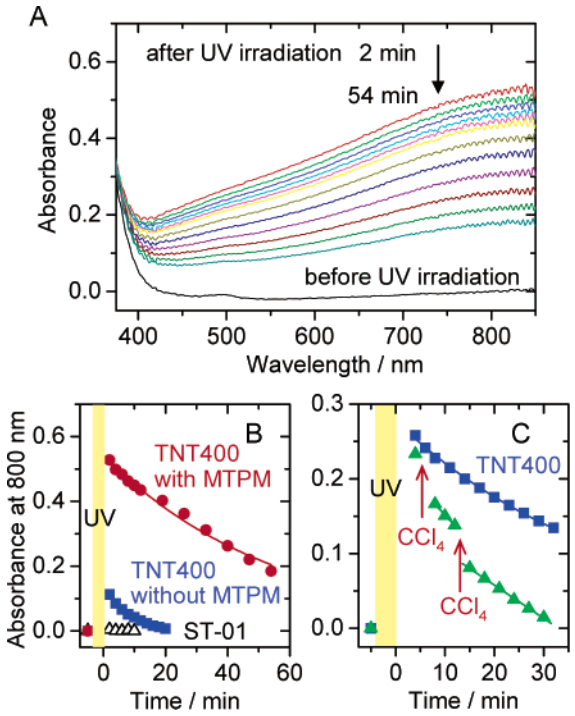

Figure 3. (A) Steady-state diffuse reflectance spectra observed for TNT-400 in aerated CH_3CN containing MTPM (10 mM) before and after the UV irradiation (365 nm, 10 mW cm^{-2}) for 4 min. (B) Time dependence of absorbance at 800 nm in the absence and presence of MTPM (10 mM) in aerated CH_3CN before and after the UV irradiation. (C) Change in absorbance for TNT-400 in Ar-saturated CH_3CN after the injection of CCl_4 (1 μL) into the suspension (2 mL) (see arrows).

of the trapped e^- in TiO_2 that absorb light throughout the visible and into the infrared region.[35,36] Figure 3A shows the steady-state diffuse reflectance spectra observed for the TNT-400 powder in aerated CH_3CN containing MTPM before and after UV irradiation (366 nm, 10 mW cm^{-2}, 4 min). The absence of the absorption band due to $MTPM^{\bullet+}$ at around 550 nm indicates that the generated $MTPM^{\bullet+}$ was already degraded. It should be noted that no detectable absorption due to the trapped e^- was observed for all nanoparticle powders in both the absence and presence of MTPM under the same conditions (Figure 3B). The significant increases in the concentration (by ~4 times) and lifetime (τ_e) (by ~7 times) of the trapped e^- by the addition of MTPM are qualitatively consistent with the experimental results obtained by the time-resolved diffuse reflectance measurements (Table 1). We also observed a bleaching of the absorption band after CCl_4 was added to the suspension in the dark, suggesting that the trapped e^- in TNT-400 can rapidly react with organic halide pollutants (Figure 3C).[37,38]

The lifetime of the radical cations plays an important role in the degradation process of organic compounds during the photocatalytic reactions.[18,19,39] It was proposed that the formation of surface-adsorbed intermediates, such as the radical cations, might increase the charge recombination and thus lower the quantum yield for degradation. A theoretical analysis of the kinetics in the photocatalytic systems taking into account the possibility that a radical cation recombines with e^- can justify this behavior.[19] Hence, the long-lived transient species such as radical cations, which originate from the one-dimensional nature of the nanotubes, should lead to the high photocatalytic degradation rate of pollutants, when compared to those for nanoparticles.

Conclusions

In conclusion, we have investigated the photocatalytic one-electron oxidation reaction of an aromatic compound during UV light irradiation of TiO_2 nanotubes and nanoparticles using time-resolved diffuse reflectance spectroscopy. Remarkably long-lived radical cations of the substrate and trapped e^- were observed for the nanotubes, when compared to those for the nanoparticles. It was also found that the trapped e^- in the nanotubes can rapidly react with CCl_4. Our findings clearly suggest that the morphology of TiO_2 plays an important role in the charge recombination dynamics between surface-bound radical cations and e^- in TiO_2.

Acknowledgment. This work has been partly supported by a Grant-in-Aid for Scientific Research (Project 17105005, Priority Area (417), 21st Century COE Research, and others) from the Ministry of Education, Culture, Sports, Science and Technology (MEXT) of Japanese Government, and by the New Energy and Industrial Technology Development Organization (NEDO).

Supporting Information Available: Figures containing the XRD spectra and TEM images of the TiO_2 powders (S1); Langmuir-type plots for MTPM (S2). Table containing equilibrium constants of adsorption and the total number of adsorption sites. This material is available free of charge via the Internet at http://pubs.acs.org.

References and Notes

(1) Kasuga, T.; Hiramatsu, M.; Hoson, A.; Sekino, T.; Nihara, K. *Adv. Mater.* **1999**, *11*, 1307.
(2) Saponjic, Z. V.; Dimitrijevic, N. M.; Tiede, D. M.; Goshe, A. J.; Zuo, X.; Chen, L. X.; Barnard, A. S.; Zapol, P.; Curtiss, L.; Rajh, T. *Adv. Mater.* **2005**, *17*, 965.
(3) Zhu, H. Y.; Lan, Y.; Gao, X. P.; Ringer, S. P.; Zheng, Z. F.; Song, D. Y.; Zhao, J. C. *J. Am. Chem. Soc.* **2005**, *127*, 6730.
(4) Armstrong, A. R.; Armstrong, G.; Canales, J.; García, R.; Bruce, P. G. *Adv. Mater.* **2005**, *17*, 862.
(5) Tokudome, H.; Miyauchi, M. *Angew. Chem., Int. Ed.* **2005**, *44*, 1974.
(6) Liu, S.; Chen, A. *Langmuir* **2005**, *21*, 8409.
(7) Du, Y.; Rabani, J. *J. Phys. Chem. B* **2003**, *107*, 11970.
(8) Adachi, M.; Murata, Y.; Okada, I.; Yoshikawa, S. *J. Electrochem. Soc.* **2003**, *150*, G488.
(9) Ngamsinlapasathian, S.; Sakulkhaemaruethai, S.; Pavasupree, S.; Kitiyanan, A.; Sreethawong, T.; Suzuki, Y.; Yoshikawa, S. *J. Photochem. Photobiol. A* **2004**, *164*, 145.
(10) Ohsaki, Y.; Masaki, N.; Kitamura, T.; Wada, Y.; Okamoto, T.; Sekino, T.; Niihara, K.; Yanagida, S. *Phys. Chem. Chem. Phys.* **2005**, *7*, 4157.
(11) Mor, G. K.; Shankar, K.; Paulose, M.; Varghese, O. K.; Grimes, C. A. *Nano Lett.* **2006**, *6*, 215.
(12) Park, J. H.; Kim, S.; Bard, A. J. *Nano Lett.* **2006**, *6*, 24.
(13) Rothenberger, G.; Moser, J.; Grätzel, M.; Serpone, N.; Sharma, D. K. *J. Am. Chem. Soc.* **1985**, *107*, 8054.
(14) Serpone, N.; Lawless, D.; Khairutdinov, R.; Pelizzetti, E. *J. Phys. Chem.* **1995**, *99*, 16655.
(15) Bahnemann, D. W.; Hilgendorff, M.; Memming, R. *J. Phys. Chem. B* **1997**, *101*, 4265.
(16) Yoshihara, T.; Katoh, R.; Furube, A.; Tamaki, Y.; Murai, M.; Hara, K.; Murata, S.; Arakawa, H.; Tachiya, M. *J. Phys. Chem. B* **2004**, *108*, 3817.
(17) Shkrob, I. A.; Sauer, M. C., Jr. *J. Phys. Chem. B* **2004**, *108*, 12497.
(18) Minero, C.; Mariella, G.; Maurino, V.; Pelizzetti, E. *Langmuir* **2000**, *16*, 2632.
(19) Minero, C. *Catal. Today* **1999**, *54*, 205.
(20) Draper, R. B.; Fox, M. A. *J. Phys. Chem.* **1990**, *94*, 4628.
(21) Draper, R. B.; Fox, M. A. *Langmuir* **1990**, *6*, 1396.
(22) Asahi, T.; Furube, A.; Fukumura, H.; Ichikawa, M.; Masuhara, H. *Rev. Sci. Instrum.* **1998**, *69*, 361.
(23) Furube, A.; Asahi, T.; Masuhara, H.; Yamashita, H.; Anpo, M. *J. Phys. Chem. B* **1999**, *103*, 3120.

(24) Tachikawa, T.; Tojo, S.; Fujitsuka, M.; Majima, T. *Langmuir* **2004**, *20*, 2753.
(25) Tachikawa, T.; Tojo, S.; Fujitsuka, M.; Majima, T. *J. Phys. Chem. B* **2004**, *108*, 5859.
(26) Tachikawa, T.; Yoshida, A.; Tojo, S.; Sugimoto, A.; Fujitsuka, M.; Majima, T. *Chem.*−*Eur. J.* **2004**, *10*, 5345.
(27) Tachikawa, T.; Tojo, S.; Kawai, K.; Endo, M.; Fujitsuka, M.; Ohno, T.; Nishijima, K.; Miyamoto, Z.; Majima, T. *J. Phys. Chem. B* **2004**, *108*, 19299.
(28) We assumed that the molar absorption coefficients of the trapped h^+s for the nanotubes and nanoparticles are the same.
(29) Haque, S. A.; Tachibana, Y.; Willis, R. L.; Moser, J. E.; Grätzel, M.; Klug, D. R.; Durrant, J. R. *J. Phys. Chem. B* **2000**, *104*, 538.
(30) Barzykin, A. V.; Tachiya, M. *J. Phys. Chem. B* **2002**, *106*, 4356.
(31) Sun, B.; Smirniotis, P. G. *Catal. Today* **2003**, *88*, 49.
(32) Lu, G.; Linsebigler, A.; Yates, J. T., Jr. *J. Phys. Chem.* **1994**, *98*, 11733.
(33) Kim, K. S.; Barteau, M. A. *Surf. Sci.* **1989**, *223*, 13.
(34) Farfan-Arribas, E.; Madix, R. J. *J. Phys. Chem. B* **2002**, *106*, 10680.
(35) Rothenberger, G.; Fitzmaurice, D.; Grätzel, M. *J. Phys. Chem.* **1992**, *96*, 5983.
(36) Serpone, N.; Texier, I.; Emeline, A. V.; Pichat, P.; Hidaka, H.; Zhao, J. *J. Photochem. Photobiol. A* **2000**, *136*, 145.
(37) Calza, P.; Minero, C.; Pelizzetti, E. *J. Chem. Soc., Faraday Trans.* **1997**, *93*, 3765.
(38) Calza, P.; Minero, C.; Pelizzetti, E. *Environ. Sci. Technol.* **1997**, *31*, 2198.
(39) Tachikawa, T.; Takai, Y.; Tojo, S.; Fujitsuka, M.; Majima, T. *Langmuir* **2006**, *22*, 893.